Site-Specific, Thiol-Mediated Conjugation of Fluorescent Probes to Cysteine-Modified Diabodies Targeting CD20 or HER2

Shannon J. Sirk,* Tove Olafsen, Bhaswati Barat, Karl B. Bauer, and Anna M. Wu

Crump Institute for Molecular Imaging, Department of Molecular and Medical Pharmacology, David Geffen School of Medicine at UCLA, Los Angeles, California 90095. Received March 24, 2008; Revised Manuscript Received October 15, 2008

Small, engineered antibody fragments such as diabodies (50 kDa noncovalent dimers of single-chain Fv fragments) are useful alternatives to their larger antibody counterparts. However, due to their size, they are more susceptible to disruption of their antigen binding sites when modified using random conjugation techniques. Previous work has demonstrated the utility of a C-terminal cysteine modification for site-specific radiolabeling of an anti-CEA diabody, resulting in the creation of a cys-diabody (CysDb). In the present work, the adaptability of the CysDb system was explored by creating two additional CysDbs: one specific for CD20 and one for HER2. Purified CysDbs of both specificities demonstrated behavior consistent with stable, covalent dimers harboring a readily reducible disulfide bond. Each CysDb was site-specifically conjugated to three different fluorophores for optical detection: the large fluorescent proteins phycoerythrin (PE) and allophycocyanin (APC), and the small fluorescent molecule Alexa Fluor488. Fluorophore-conjugated CysDbs bound specifically to their targets in both antigen systems and with each different fluorescent tag as determined by flow cytometry. *In vitro* specific antigen binding was observed in the presence of a mixture of specific and nonspecifically conjugated CysDbs. Conjugates retained both specificity and fluorescence, demonstrating the successful expansion of the CysDb repertoire to new targets and to new site-specific conjugation possibilities.

INTRODUCTION

Monoclonal antibodies (mAbs) comprise a unique class of tumor targeting agents capable of specific recognition of cell surface antigens, including cancer biomarkers. Many therapeutic mAbs have been used to target and treat a wide range of diseases, including breast cancer, lymphoma, colorectal cancer, and leukemia (*1*). When conjugated to radionuclides, antibody derivatives specific for cancer biomarkers can be employed for tumor detection using imaging methods such as positron emission tomography (PET) (*2*−*4*). MAbs armed with therapeutic radionuclides or other cytotoxic agents have been used to deliver targeted toxicity to a tumor while minimizing damage to healthy tissue (*5, 6*).

Intact mAbs are highly specific targeting agents but are not suited for every application due to their large size and full Fc domain. Engineered antibody fragments harness the specificity of the variable domains while modifying or deleting the constant domains to suit the intended targeting need (*7, 8*). Single-chain Fvs (scFvs), consisting of the variable light (V_L) and variable heavy (V_H) domains joined by an amino acid linker, are the smallest antibody fragments that still retain specificity and are commonly used antigen-specific probes (*9*−*11*). ScFv linker length influences fragment multimerization, with shorter linkers (3−12 residues) supporting the formation of bivalent diabodies (Dbs) (*12*). Compared to scFvs, Dbs demonstrate superior binding *in vitro* and improved tumor accumulation *in vivo* due to increased avidity and therefore increased functional affinity (*13*).

Targeting applications regularly involve labeling antibodies and antibody fragments, often with a radionuclide. Common techniques involve conjugation via random tyrosine or lysine residues (*14, 15*). Intact antibodies (150 kDa) are large enough to offer several sites that will not disrupt antigen binding when conjugated to a labeling agent. At a fraction of the size of intact antibodies, Dbs (50 kDa) have fewer available conjugation sites, and it is therefore more likely that conjugation will disrupt antigen binding or overall conformation and efficacy of the molecule as a tumor targeting agent.

To address this problem, methods for site-specifically labeling Dbs and bypassing potential adverse effects of random conjugation have been pursued. The addition of C-terminal cysteinyl peptides was originally explored as a method to induce dimerization of scFv molecules (*16, 17*) and provide a defined site for radiometal chelation (*18*). Site-specific PEGylation has been used to adjust the circulating half-life of cysteine-modified scFvs (*19*), and liposomes have been coupled via thiol chemistry to scFvs targeting tumor biomarkers and tumor stromal cells (*20, 21*).

Crystallographic analysis of an anti-carcinoembryonic antigen (CEA) Db revealed that the antigen binding sites are located on opposite sides from the C-termini of the V_H domains (*22*). An anti-CEA Db with a cysteine residue incorporated at the C-terminus of the V_H domain of each scFv monomer was created (CysDb) and expressed in mammalian cell culture, spontaneously yielding stable covalent dimers (*23*). Anti-CEA CysDbs demonstrated excellent binding *in vitro* and, following site-specific chelate conjugation and radiometal labeling, specifically targeted CEA-expressing tumor xenografts in a microPET mouse model (*23*).

On the basis of this initial success, the CysDb format was extended to two additional cancer targets—CD20 (lymphoma) and HER2 (breast cancer). CD20 and HER2 were chosen as candidate antigen systems because there are pre-existing, well-characterized therapeutic antibodies (rituximab and trasuzumab) specific for these targets. Functional CysDbs of both specificities were produced and characterized. Both CysDbs retained specific antigen binding following site-specific conjugation to three different fluorophores. Bifunctionality of each conjugate is

* Author to whom correspondence should be addressed. ssirk@mednet.ucla.edu, 700 Westwood Plaza, Crump A420, Los Angeles, CA 90095, Telephone (310) 267-2819, Fax (310) 206-8975.

10.1021/bc800113v CCC: $40.75
Published on Web 11/18/2008

demonstrated through the observed antigen specificity of each CysDb as well as the unique fluorescence profile of each attached fluorophore. Successful expansion of the C-terminal cysteine modification to two new specificities supports the utility of the CysDb format as a generalizable platform for site-specific conjugation of tumor targeting molecules with functional payloads.

EXPERIMENTAL PROCEDURES

Design of Cysteine-Modified Diabodies. Diabodies were constructed from existing gene constructs containing variable regions recognizing HER2 (*4*) or CD20 (Olafsen et al. [abstr.], *J. Nucl. Med.* 47:48P, 2006). Overlap-extension PCR and site-directed mutagenesis (QuikChange XL, Stratagene) were used to create CysDb genes with a five amino acid linker (SGGGG) between the variable light (V_L) and variable heavy (V_H) domains and a C-terminal cysteine modification (GGC) to give the final CysDb construct: (V_L-SGGGG-V_H-GG**C**) in the pEE12 mammalian expression vector (*24*). All constructs were confirmed by DNA sequencing.

Mammalian Expression, Selection, and Purification. 2.5×10^6 NS0 mouse myeloma cells (Sigma) were transfected by electroporation with 10 μg linearized plasmid DNA and selected in glutamine-deficient DMEM (Mediatech Inc.) as described (*24*). Transfectants were screened for CysDb expression by assaying cell culture supernatant by ELISA and/or SDS-PAGE using precast 4−20% gels (Bio-Rad).

ELISA. For anti-CD20 CysDb ELISA, microtiter plate wells were coated with 100 μL (2 μg/mL) goat anti-mouse Fab (Sigma), then blocked with 1% BSA. 100 μL cell culture supernatant was assayed, and anti-CD20 CysDb was detected with 100 μL (0.4 μg/mL) alkaline phosphatase (AP)-conjugated goat anti-mouse Fab (Jackson Immunolabs). Signal was developed using phosphatase substrate tablets (Sigma), and absorbance was detected at 405 nm using a microplate reader (Tecan). The same procedure was performed for anti-HER2 CysDb ELISA, except using Protein L (Sigma) for coating wells and Protein L-horse radish peroxidase (HRP) (Sigma) for detection. Signal was developed with CN/DAB Substrate Kit (Pierce) and analyzed visually for black precipitate.

Gel Electrophoresis and Immunoblotting. SDS-PAGE gels were run with 30 μL cell culture supernatant and either stained with Microwave Blue (Protiga) or transferred to nitrocellulose membrane for Western analysis. Samples were run under both reducing (100 mM DTT) and nonreducing conditions. Anti-CD20 CysDb was detected on Western blot with 0.4 μg/mL goat anti-mouse Fab-AP (Jackson Immunolabs), and color was developed with NBT/BCIP substrate (Promega). Anti-HER2 CysDb was detected on Western blot by Protein L-HRP (Sigma) and color was developed with CN/DAB Substrate Kit (Pierce).

Purification. Clones showing the highest expression were expanded into triple flasks (Corning), and approximately 700 mL cell culture supernatant was collected and filtered on a polyethersulfone (PES) membrane (Corning). Supernatant was loaded onto a Protein L column (Pierce) with a bed volume of 1 mL at a flow rate of 0.4 mL/min in PBS using an ÄKTA Purifier (GE Healthcare Life Sciences). Bound protein was eluted with 0.1 M glycine, pH 2.5, over 20 column volumes. Eluted fractions were neutralized upon collection in 5% final volume 2 M Tris, pH 8.0. Fractions containing protein were identified by SDS-PAGE and combined. Buffer was exchanged to PBS, protein was concentrated using a spin column (Vivaspin 20, 10 kDa cutoff), and protein was stored at 4 °C.

Characterization of Purified CysDbs. Purified, concentrated protein was analyzed by SDS-PAGE followed by Microwave Blue gel staining or Western blot analysis as described above. All molecular weights were approximated by comparison to Kaleidoscope prestained molecular weight standard (Bio-Rad) and a previously characterized anti-CEA CysDb with a known molecular weight of 55 kDa. CysDbs were also subjected to size-exclusion chromatography on a Superdex 75 column (GE Healthcare Life Sciences) in PBS at a flow rate of 0.5 mL/min over one column volume (24 mL) on an ÄKTA Purifier. Protein purity was estimated from size exclusion chromatography data. Anti-CD20 CysDb (only) was analyzed for specific binding by indirect flow cytometry, described below.

Site-Specific Fluorescent Labeling. Cys-diabodies were site-specifically conjugated using thiol chemistry to three different fluorophores: phycoerythrin activated with succinimidyl 4-[*N*-maleimidomethyl]-cyclohexane-1-carboxylate (PE-SMCC, 240 kDa, Prozyme), allophycocyanin (APC)-SMCC (104 kDa, Prozyme), or Alexa Fluor 488 C_5-maleimide (A488, 720 Da, Invitrogen). Each CysDb was conjugated to each fluorophore individually, resulting in six conjugates (3 fluorescent tags × 2 CysDb specificities). Mock conjugation controls were treated under the same conditions, except with no CysDb added. Following the Phycolink conjugation kit guidelines (Prozyme), 150 μg of CysDb in 60 μL PBS was incubated at room temperature with 16 mM DTT for 30 min to reduce disulfide bonds. DTT was removed from reduction reactions using a Micro Bio-Spin 6 chromatography column (Bio-Rad), equilibrated with Exchange Buffer (50 mM MES, 2 mM EDTA, pH 6.0). Reduced CysDb was then incubated with 240 μg activated PE or APC (10 mg/mL in 50 mM MES, 2 mM EDTA, pH 6.0, with 1 μg/mL pentachlorophenol [preservative]), or 12 μg A488 (1 μg/mL, 1.4 mM in water). Molar ratios in the conjugation reactions were approximately 1:3, 1:1.25, and 5.6:1 for PE/CysDb, APC/CysDb, and A488/CysDb, respectively. Addition of fluorophore was followed by incubation in the dark at room temperature for 1 h with occasional mixing. Remaining free sulfhydryls were then blocked with 5.1 μg *N*-ethylmaleimide (NEM, 10 mg/mL in DMSO, Sigma). Reactions were wrapped in foil, incubated at room temperature with occasional mixing for 30 min, and then applied to new spin columns equilibrated with Storage Buffer (10 mM Tris-HCl, 150 mM NaCl, pH 8.2). Fluorophore-conjugated CysDbs were stored in 1.5 mL Eppendorf tubes at 4 °C, wrapped in aluminum foil. Protein yield and conjugation ratios were determined using a UV/visible spectrophotomer (Ultrospec 1100 Pro, GE Healthcare Life Sciences) to measure absorption at 280 and at the peak absorption wavelength of each flurophore.

Flow Cytometry. Flow cytometry was used to evaluate binding of CysDbs to cell-surface antigen before (anti-CD20 CysDb only) and after site-specific fluorescent labeling. Unconjugated anti-CD20 CysDb was tested on 38C13 mouse myeloma cells (ATCC #HB-132) transfected with human CD20 (*25*). Conjugated CysDbs were tested on SKW 6.4 (human B cell lymphoma, CD20-positive, ATCC #TIB-215), Daudi (human B cell lymphoma, CD20-positive, ATCC #CCL-213), and MCF-7 $HER2^+$ (human breast cancer, HER2-transfected, gift of Dr. Dennis Slamon, UCLA School of Medicine) (*26*). Cells were harvested and resuspended in PBS/1% FBS to a final concentration of 1×10^6 cells/mL. For each reaction, 5×10^5 cells (500 μL) were incubated with fluorophore-conjugated CysDb (0.5 or 5 μL) for 1 h on ice with occasional mixing.

38C13-$CD20^+$ cells were incubated first with unconjugated anti-CD20 CysDb, followed by PE-conjugated anti-mouse Fab secondary antibody (Jackson Immunolabs). SKW6.4 cells were incubated with PE-conjugated anti-CD20 CysDb only.

Each fluorescent CysDb and each mock conjugate was incubated in separate reactions with Daudi cells and MCF7-$HER2^+$ cells. Experiments were performed with 0.5 μL (low concentration sample) or 5 μL (high concentration sample) of conjugated CysDb or mock-conjugated dye. Each fluorescent

CysDb was also assayed for specific binding to either Daudi (anti-CD20 CysDbs) or MCF7-HER2$^+$ (anti-HER2 CysDbs) in the presence of other CysDbs. Mixtures were composed of one antigen-specific and two antigen-nonspecific fluorescent conjugates, with every combination represented. Each fluorescent CysDb (3 μL) was incubated with its target cell type in the presence of the other two (nonspecific) CysDb (3 μL each conjugate). Positive control samples were incubated with either anti-CD20 scFvFc (Olafsen et al. [abstr.], *J. Nucl. Med.* 47: 48P, 2006) for Daudi or anti-HER2 scFvFc (*4*) for MCF7-HER2$^+$ cells, and then washed and incubated with each of three fluorescently labeled anti-human-IgG-Fc-specific secondary antibodies (PE- and APC-conjugated, Jackson Immunolabs; Alexafluor 488-conjugated, Molecular Probes). All samples were then washed with PBS/1% FBS, resuspended in 500 μL PBS/1%FBS, filtered, and analyzed on a modified FACScan flow cytometer using *CellQuest* software (BD Biosciences). Fluorescence of 10 000 gated viable cells was collected simultaneously in 3 channels for each sample. A488 signal (519 nm emission wavelength) was detected in FL1, PE signal (578 nm emission wavelength) was detected in FL2, and APC signal (661 nm emission wavelength) was detected in FL4.

RESULTS

Design and Construction of CysDbs. C-terminal GGC modifications were added to anti-HER2 and anti-CD20 scFv gene constructs as shown (Figure 1). Anti-CD20 CysDb gene was constructed from an existing anti-CD20 single chain variable fragment gene (scFv, V_L-SGGGG-V_H), composed of rituximab (Rituxan, Genentech) mouse variable regions (Olafsen et al. [abstr.], *J. Nucl. Med.* 47:48P, 2006). Anti-HER2 CysDb gene was constructed from trastuzumab (Herceptin, Genentech) variable regions, from an existing minibody gene (*4*). The scFv orientation and linker of the anti-HER2 minibody were as follows: V_L-GSTSGGGSGGGSGGGGSS-V_H. Overlap extension PCR was used to shorten the 18 amino acid linker in the anti-HER2 scFv gene to a 5 amino acid linker (SGGGG).

Mammalian Expression. Following transfection of NS0 cells with either anti-CD20 or anti-HER2 CysDb gene construct, positive clones were identified by growth of single colonies in microtiter plates. CysDb-expressing transfectants were screened by ELISA and Western blot (data not shown). Color development verified positive clones by ELISA and allowed ranking of relative expression levels within this group. Bands on Western blots were detected at approximately 50 kDa (nonreduced) and 25 kDa (reduced), providing confirmation of the correct size of both dimer and monomeric subunit forms of the protein.

Purification. Clones expressing anti-CD20 CysDb and clones expressing anti-HER2 CysDb were expanded and CysDb was purified from the media by affinity chromatography on a Protein L column. Final protein yields were 1.6 mg/L of culture supernatant for anti-CD20 CysDb and 3.0 mg/L of culture supernatant for anti-HER2 CysDb. Purities of >99% for anti-CD20 CysDb and >90% for anti-HER2 CysDb were determined from size exclusion chromatography data.

Characterization of Purified CysDbs. *Gel Electrophoresis and Immunoblotting.* SDS-PAGE analysis demonstrated correct size and covalent dimerization of purified CysDbs. Under nonreducing conditions, both proteins migrated near the expected molecular weights of approximately 50 kDa, verifying a population of covalently dimerized molecules in the final purified product. Under reducing conditions, CysDbs migrated at approximately 25 kDa, consistent with the expected scFv monomer (Figure 2). Purified CysDbs were specifically detected by Western blot at approximately 50 kDa (nonreduced) and approximately 25 kDa (reduced) (data not shown).

Size Exclusion Chromatography. Characterization of purified CysDbs by size-exclusion chromatography resulted in elution profiles similar to each other and to previously characterized diabodies (Figure 3). Anti-CD20 CysDb (25.2 min) and anti-HER2 CysDb (22.5 min) both eluted at times similar to the previously characterized anti-CEA CysDb (21.5 min) (*23*) and anti-CD20 Db (23.7 min) (T. Olafsen, unpublished). Anti-CD20 CysDb eluted slightly later than its parental, non-cysteine-modified diabody, suggesting a more compact form of the protein, as expected with covalent dimerization (*23*). Anti-CD20 CysDb eluted later than either of the other CysDbs, consistent with its apparent smaller size as seen by SDS-PAGE (Figure 2).

Flow Cytometry. Specific antigen binding was demonstrated for anti-CD20 CysDb by indirect flow cytometry. Fluorescence of gated viable CD20$^+$ cells showed binding comparable to that of parental, non-cysteine-modified anti-CD20 diabody (data not shown).

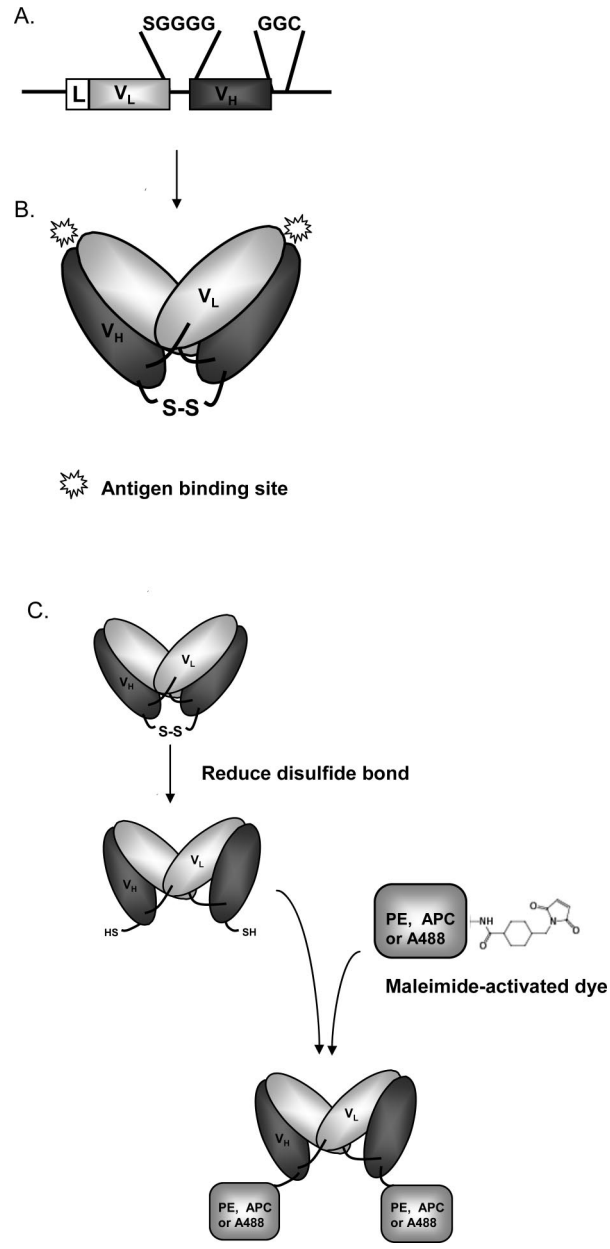

Figure 1. Schematic representation of CysDb. (A) Gene assembly for anti-CD20 and anti-HER2 CysDb (scFv monomer) with 5-aa linker and cysteine modification shown (L, leader sequence for secretion). (B) CysDb with antigen binding sites indicated by starbursts. CysDb is shown in covalent dimer form, with disulfide bond in the predicted location. (C) Conjugation reaction linking cys-diabody to fluorescent probe.

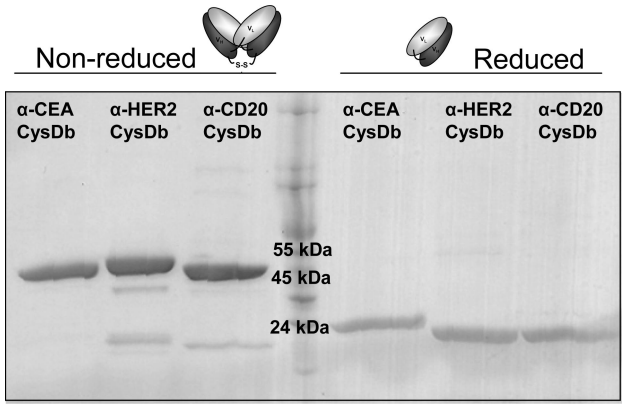

Figure 2. SDS-PAGE of three CysDbs under nonreducing (left) and reducing (right) conditions. Previously characterized anti-CEA CysDb shown for comparison purposes. Nonreduced samples migrate at expected size for covalent dimer (50 kDa), and reduced samples migrate at expected size for monomeric scFv (25 kDa).

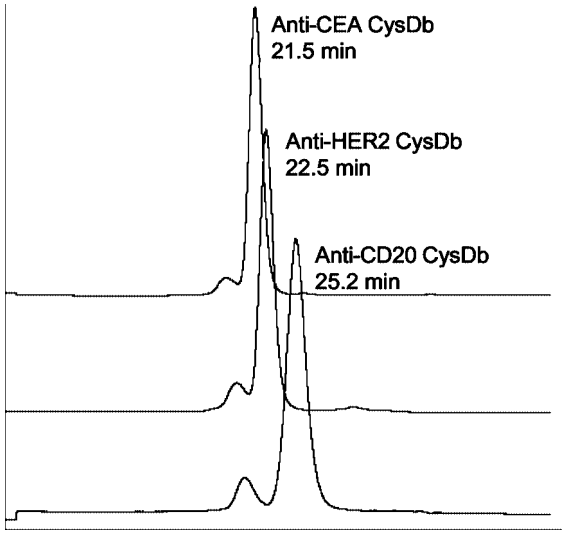

Figure 3. Size exclusion chromatography of cys-diabodies on Superdex 75 column. Previously characterized anti-CEA CysDb shown for comparison purposes.

Site-Specific Fluorescent Labeling and Specific Binding of Conjugated CysDbs. *Single-Channel Flow Cytometry.* Anti-CD20 CysDbs site-specifically conjugated to the fluorescent dyes PE, APC, or A488 demonstrated specific binding to CD20-positive Daudi cells and not to CD20-negative MCF7-HER2$^+$ cells (Figure 4). Quantities of APC and PE used were half of that suggested in the manufacturer's guidelines, as this modification yielded comparable conjugation efficiency in our hands and conserved reagent. Product guidelines for A488 recommend 10−20 mol of dye per mole of protein when conjugating thiol-reactive probes (Invitrogen). A final value of 5.6 mol of A488 C_5-maleimide per mole of CysDb was used in an attempt to reduce excessive background from unconjugated dye. Dye/protein ratios were calculated for A488 batches only, as this was the only nonprotein fluorophore and therefore gave more consistent quantitative results. The molar ratio of A488/CysDb was calculated to be 2:1.

Single-channel experiments showed binding to Daudi cells of each of the three fluorescent conjugates of anti-CD20 CysDb (Figure 4A). Mock-conjugated fluorophore background showed minimal shift in FL1, FL2 or FL4 compared to the antigen-specific binding shift of the CysDb. PE-labeled anti-CD20 CysDb also demonstrated specific binding to an additional CD20-positive cell line, SKW 6.4, by flow cytometry (data not shown). All three anti-CD20 CysDb conjugates showed a concentration-dependent shift in fluorescence from the low to the high concentration samples, with the APC version exhibiting a higher mean fluorescence in general, across all experiments performed (Figure 4B). All three anti-CD20 CysDb conjugates showed minimal nonspecific background binding to CD20-negative MCF7-HER2$^+$ cells (Figure 4C).

Analogous results were seen with PE-, APC-, and A488-conjugated anti-HER2 CysDbs. All three conjugates showed specific binding to MCF7-HER2$^+$ cells. Fluorescence shifts were seen in the expected channels for each of the conjugated CysDbs, but not for the mock-conjugated dye (Figure 5A). Cells incubated with a low concentration of PE- and APC-conjugated anti-HER2 CysDb showed very little difference in mean fluorescence intensity compared with cells incubated with a high concentration of these CysDbs (Figure 5B). When incubated with HER2-negative Daudi cells, fluorescently conjugated anti-HER2 CysDbs showed minimal background binding (Figure 5C). PE-labeled anti-HER2 CysDb also showed no binding to HER2-negative, CD20-positive SKW 6.4 cells by flow cytometry (data not shown).

Multiple-Channel Flow Cytometry. Figure 6A shows representative plots of three-channel flow cytometry experiments in which Daudi cells were incubated with a cocktail of three different CysDb conjugates: one anti-CD20 CysDb and two anti-HER2 CysDbs, each conjugated to a different fluorophore. Each of the three anti-CD20 CysDb fluorescent conjugates was tested in combination with two anti-HER2 CysDb fluorescent conjugates. For anti-CD20 CysDb-PE, specific binding to Daudi cells was demonstrated by signal in FL2 (upward shift). Minimal background signal was detected in FL4 or FL1 from either APC- or A488-conjugated anti-HER2 CysDb, respectively, as seen by a lack of rightward shift in fluorescence (Figure 6A). Similar results were seen when APC- or A488-conjugated anti-CD20 CysDb was incubated with Daudi cells in a three-conjugate mix with anti-HER2 CysDb and subjected to flow cytometric analysis in all three fluorescence channels (Figure 6B).

Parallel experiments were run with MCF7-HER2$^+$ cells which showed specific binding of conjugated anti-HER2 CysDb when mixed with anti-CD20 CysDb conjugates in three-conjugate cocktail experiments as described above. Figure 6C shows a representative plot demonstrating specific detection in FL2 of PE-conjugated anti-HER2 CysDb bound to MCF7-HER2$^+$ cells, while minimal background signal of APC- or A488-conjugated anti-CD20 CysDb was seen in FL4 or FL1, respectively. Similar results were seen for the other combinations of fluorescent conjugates. For each sample, nearly 100% of the signal was in the channel specific to the anti-HER2 conjugate being detected, while fluorescence from the nonspecific anti-CD20 CysDb was not seen, with the exception of a slightly higher background from the APC-conjugated anti-CD20 CysDb (Figure 6D).

DISCUSSION

Cysteine-modified diabodies were engineered for use as site-specifically modifiable, cancer biomarker-specific antibody fragments. The decision to place the cysteine modification at the C-terminus of the V_L-linker-V_H construct was based on previous success with a similar modification which generated the T84.66 anti-CEA CysDb (*23*). The current work extends the CysDb format from CEA to two additional antibodies recoginizing CD20 and HER2, demonstrating that this format is general. Since the C-termini of the diabody subunits are physically opposite from the antigen-binding sites on the CysDb, following reduction, any further modification to the free sulfhydryls should not interfere with binding activity (*23*). Purified CysDb exists as a stable covalent dimer until subjected to reducing conditions, demonstrating a system with simple and

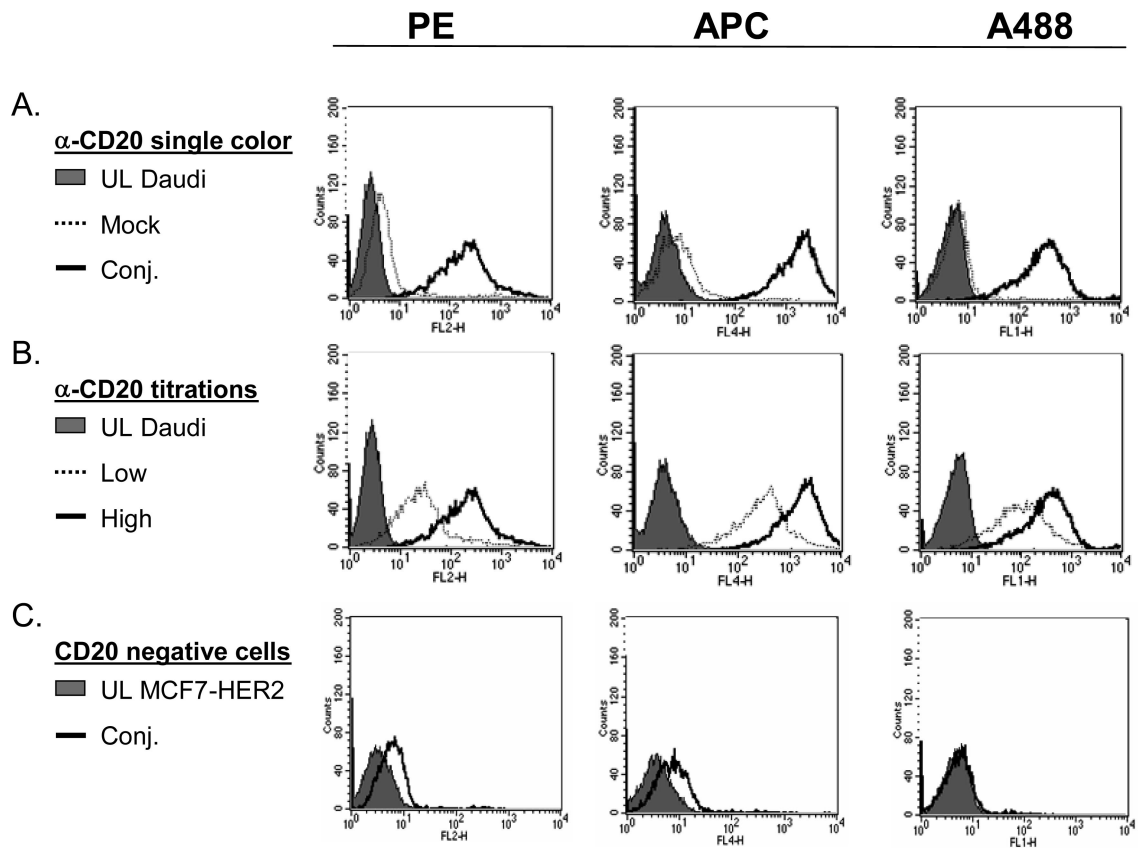

Figure 4. Flow cytometry of single-channel labeling with dye-conjugated anti-CD20 CysDb. Unlabeled cells (UL) shown in solid gray. (A) Three channels of dye-conjugated anti-CD20 CysDb (Conj., thick line) and mock conjugated dye (Mock, dotted line) demonstrating minimal background from nonspecific binding of free dye molecules to $CD20^+$ Daudi cells. (B) Three channels of low (0.5 μL, dotted line) and high (5 μL, thick line) concentrations of dye-conjugated anti-CD20 CysDb demonstrating concentration-dependent shift in mean fluorescence with increasing quantities of conjugated CysDb. (C) Three channels of dye-conjugated anti-CD20 CysDb (Conj., thick line) with minimal binding to CD20-negative MCF7-$HER2^+$ cells, demonstrating antigen-specificity of binding.

reliable control over the availability of free sulfhydryls for thiol-specific conjugation.

The presence of C-terminal cysteine residues clearly induces efficient disulfide bridge formation and a compact overall conformation. Olafsen et al. first observed that the cysteine modification and subsequent disulfide bridge formation caused an anti-CEA CysDb to appear more condensed than the parental diabody (*23*). We also found that, for the two diabody/CysDb pairs examined (anti-CD20, anti-HER2), the cysteine-modified version consistently eluted later on size exclusion chromatography compared to the native diabody (data not shown), consistent with a more closed conformation of the covalent dimer. Elution time by size exclusion appears to be an innate property of each CysDb (Figure 3) and was reproducible among purified batches of the same CysDb. The anti-HER2 CysDb and the anti-CD20 CysDb both have a predicted molecular weight of 50 kDa, although the anti-CD20 CysDb consistently eluted later by size exclusion chromatography (Figure 3). Observed differences in elution times may reflect the sequence difference in the binding sites, as well as the fact that the rituximab framework is murine whereas trastuzumab is humanized. Minor differences in migration were also observed on SDS-PAGE (Figure 2), indicating that mobility was influenced by primary sequence as well as molecular weight.

Reduction of the CysDb disulfide bridges provided a flexible and reproducible approach for site-specific conjugation. Fluorescent dyes spanning a molecular weight range from subkilodalton (A488) to several hundred kilodaltons (PE, APC) were readily coupled to the CD20- and HER2-specific CysDbs to yield six distinct bifunctional conjugates. At the same time, these conjugates retained the ability to bind to antigen, indicating that the internal disulfide bridges in the V regions, characteristic of the conserved immunoglobulin fold, were not disrupted. In addition, spectrophotometric quantitation of the molar conjugation ratio indicated ~2 dye molecules per diabody, consistent with conjugation of fluorophores only onto the two most easily accessible sulfhydryls, at the C-termini.

Fluorescent antibody fragments are regularly used for *in vitro* detection applications and *in vivo* studies in small animals for noninvasive monitoring and radiation-free imaging (*29*). Multichannel flow cytometry experiments in the current work demonstrated antigen-specific binding with the use of a cocktail of fluorescent CysDbs with a spectrum of labels, supporting this format as a robust and easily interchangeable targeting molecule. Increasingly, optically labeled antibody fragments are being used for fluorescence-guided surgery and intraoperative visualization of metastastes (*30*). CysDbs are promising for this application, as their small size should allow them to penetrate a tumor more deeply than a larger, intact antibody. Optical detection and diagnosis using a cocktail of CysDbs recognizing a set of different tumor biomarkers could provide a means for simultaneous evaluation of multiple proteins, subject to the known limitations of detection of visible light in tissues and living organisms.

The CysDb format provides a general approach for combining minimal antibody binding domains with a variety of functional moieties. Previously, the cysteine modification was used for site-specific conjugation of the macrocyclic metal chelator DOTA(1,4,7,10-tetraazacyclododecane-1,4,7,10-tetraacetic acid), enabling radiolabeling of the anti-CEA CysDb with ^{64}Cu for microPET detection of CEA-expressing LS174T xenografts in mice (*23*). In addition to radiolabeling, site-specific PEGylation

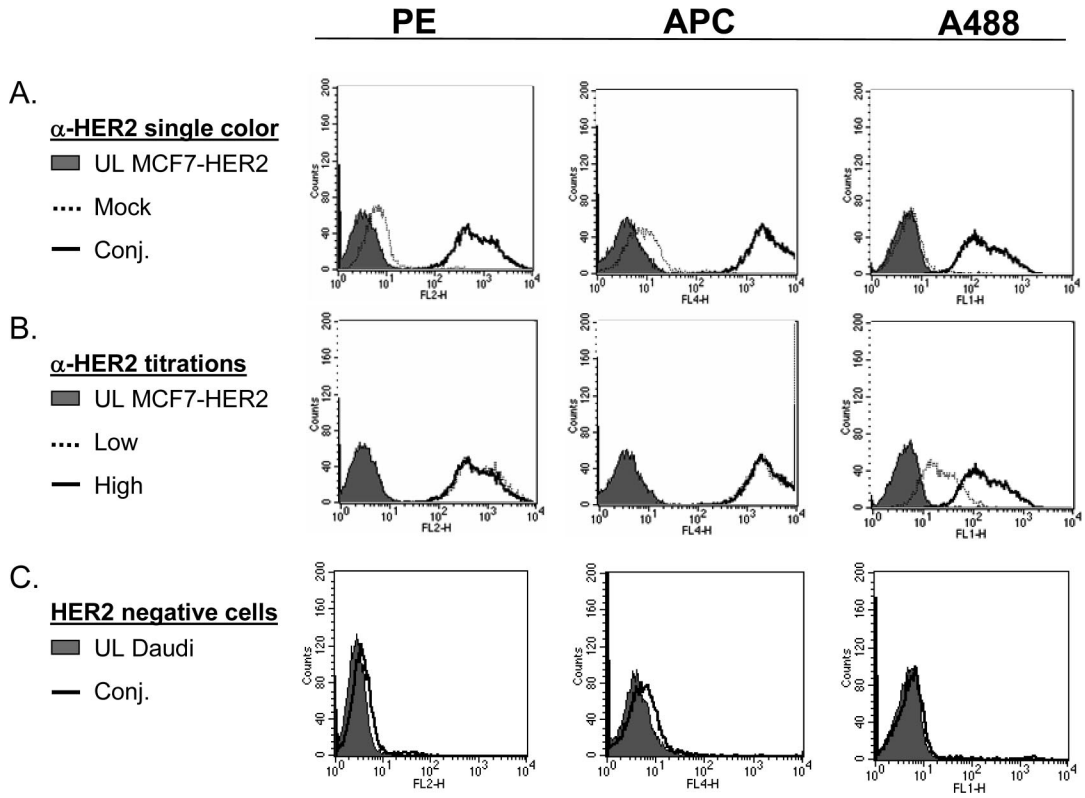

Figure 5. Flow cytometry of single-channel labeling with dye-conjugated anti-HER2 CysDb. Unlabeled cells (UL) shown in solid gray. (A) Three colors of dye-conjugated anti-HER2 CysDb (Conj., thick line) and mock conjugated dye (Mock, dotted line) demonstrating minimal background from nonspecific binding of free dye molecules to MCF7-HER2^{+} cells. (B) Three channels of low (0.5 μL, dotted line) and high (5 μL, thick line) concentrations of dye-conjugated anti-HER2 CysDb demonstrating concentration-dependent shift in mean fluorescence with increasing quantities of conjugated CysDb. (C) Three channels of dye-conjugated anti-HER2 CysDb (Conj., solid line) with minimal binding to HER2-negative Daudi cells, demonstrating antigen-specificity of binding.

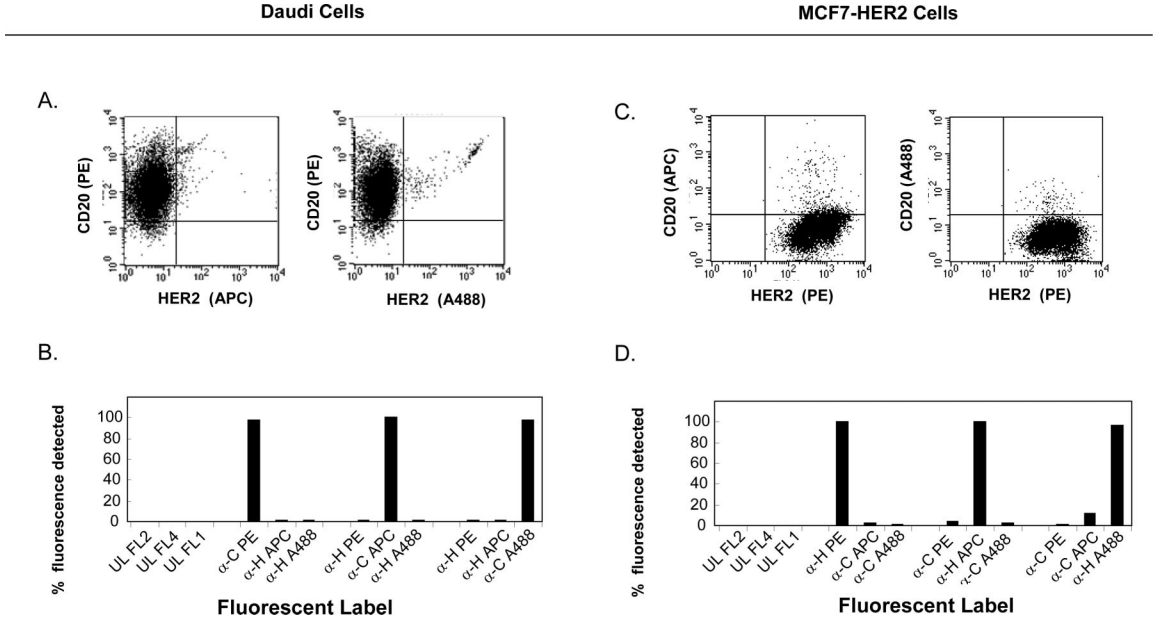

Figure 6. Flow cytometry of three-channel labeling of Daudi (A and B) and MCF7-HER2 (C and D) cells with antigen-specific and isotype control dye-conjugated CysDbs. (A) Two representative plots from three-channel experiments demonstrating detection in FL2 of specific binding of PE-conjugated anti-CD20 CysDb with minimal signal in FL1 or FL4 from co-incubated APC- or A488-conjugated anti-HER2 CysDbs, respectively. (B) Bar graph presenting compiled results of all three-channel labeling experiments on Daudi cells, demonstrating consistent, specific detection of all three dye-conjugated anti-CD20 CysDbs and minimal background from nonspecific binding of dye-conjugated anti-HER2 CysDbs. Analogous experiments were performed with dye-conjugated anti-HER2 CysDbs on MCF7-HER2 cells, using dye-conjugated anti-CD20 CysDbs as isotype controls (C,D).

of cysteine-modified scFvs or Dbs has been used to modify the pharmacokinetics of these small antibody formats (*31*). The incremental addition of several kilodaltons of PEG increases serum residence time in a predictable, size-dependent manner (*32*). The ability of the diabodies to accept large payloads is not limited to inert substances such as PEG. Venisnik et al.

fused bioluminescent enzymes to an anti-CEA diabody, demonstrating the ability of the diabody to deliver *Renilla* luciferase and *Gaussia* luciferase to a CEA-expressing tumor *in vivo* (*33, 34*). The success of this fusion protein approach confirms that relatively large functional groups can be linked to the C-termini of diabodies while maintaining binding and targeting capabilities. However, the fusion protein strategy lacks the flexibility of the CysDb approach, as each individual combination requires engineering and expression of a distinct construct.

CysDbs are especially attractive for nanotechnology applications, due to their overall size (diabody dimensions are approximately 5 nm × 7 nm) (*22*), bivalency, and capability for oriented coupling. Nanoparticles such as quantum dots, iron oxide particles, dendrimers, liposomes, and others are emerging as a distinct class of reagents with significant potential for *in vivo* applications (*21, 35, 36*). Several nanoparticles have been developed for use in imaging and therapy, but a general challenge in the field remains the need for targeted *in vivo* delivery (*37*). Oriented conjugation using antigen-specific CysDbs may provide one solution. For example, CysDbs have recently been conjugated to quantum dots, demonstrating specific binding by flow cytomety and confocal microscopy (Barat, B., Sirk, S., et al., submitted). Site-specific thiol coupling of CysDbs to nanoparticles or nanosensor substrates would automatically orient the antigen-binding domains outward to enable interaction with molecules of interest. Furthermore, attachment of CysDbs to nanodevices or nanowires should also shorten the overall interaction distances compared to coupling of intact antibodies (*38, 39*).

These studies show the utility of the CysDb platform as a simple C-terminal modification with the potential to be applied to any existing scFv or diabody. Six fluorescent antibody fragments were produced, demonstrating the versatility and reproducibility of the system. CysDbs are promising as targeting agents for *in vivo* delivery due to their small size and retention of bivalent binding. CysDbs represent a robust and simple method for reliable, site-specific, and oriented conjugation of tumor-targeting proteins to cargo of a range of size and function.

ACKNOWLEDGMENT

This work was supported by the Research Training in Pharmacological Sciences Training Grant (NIH T32 GM008652) and National Cancer Institute grants P50 CA107399, U54 CA119367, R01 EB000312, and P50086306. Flow cytometry was performed in the UCLA Jonsson Comprehensive Cancer Center and Center for AIDS Research Flow Cytometry Core Facility (NIH CA16042 and AI28697). A. W. is a member of the Jonsson Comprehensive Cancer Center (CA16042). The authors thank Roland Remenyi for experimental contributions and Katelyn McCabe for careful review of the manuscript.

LITERATURE CITED

(1) Adams, G. P., and Weiner, L. M. (2005) Monoclonal antibody therapy of cancer. *Nat. Biotechnol. 23*, 1147–57.

(2) Robinson, M. K., Doss, M., Shaller, C., Narayanan, D., Marks, J. D., Adler, L. P., Gonzalez Trotter, D. E., and Adams, G. P. (2005) Quantitative immuno-positron emission tomography imaging of HER2-positive tumor xenografts with an iodine-124 labeled anti-HER2 diabody. *Cancer Res. 65*, 1471–8.

(3) Cai, W., Olafsen, T., Zhang, X., Cao, Q., Gambhir, S. S., Williams, L. E., Wu, A. M., and Chen, X. (2007) PET imaging of colorectal cancer in xenograft-bearing mice by use of an 18F-labeled T84.66 anti-carcinoembryonic antigen diabody. *J. Nucl. Med. 48*, 304–10.

(4) Olafsen, T., Kenanova, V. E., Sundaresan, G., Anderson, A. L., Crow, D., Yazaki, P. J., Li, L., Press, M. F., Gambhir, S. S., Williams, L. E., Wong, J. Y., Raubitschek, A. A., Shively, J. E., and Wu, A. M. (2005) Optimizing radiolabeled engineered anti-p185HER2 antibody fragments for in vivo imaging. *Cancer Res. 65*, 5907–16.

(5) Sharkey, R. M., and Goldenberg, D. M. (2006) Targeted therapy of cancer: new prospects for antibodies and immunoconjugates. *CA Cancer J. Clin. 56*, 226–43.

(6) Wu, A. M., and Senter, P. D. (2005) Arming antibodies: prospects and challenges for immunoconjugates. *Nat. Biotechnol. 23*, 1137–46.

(7) Wu, A. M., and Yazaki, P. J. (2000) Designer genes: recombinant antibody fragments for biological imaging. *Q. J. Nucl. Med. 44*, 268–83.

(8) Olafsen, T., Kenanova, V. E., and Wu, A. M. (2006) Tunable pharmacokinetics: modifying the in vivo half-life of antibodies by directed mutagenesis of the Fc fragment. *Nat. Protoc. 1*, 2048–60.

(9) Albrecht, H., Denardo, G. L., and Denardo, S. J. (2007) Development of anti-MUC1 di-scFvs for molecular targeting of epithelial cancers, such as breast and prostate cancers. *Q. J. Nucl. Med. Mol. Imaging 51*, 304–13.

(10) Huston, J. S., Levinson, D., Mudgett-Hunter, M., Tai, M. S., Novotny, J., Margolies, M. N., Ridge, R. J., Bruccoleri, R. E., Haber, E., and Crea, R. (1988) Protein engineering of antibody binding sites: recovery of specific activity in an anti-digoxin single-chain Fv analogue produced in *Escherichia coli*. *Proc. Natl. Acad. Sci. U.S.A. 85*, 5879–83.

(11) Uchino, J., Takayama, K., Harada, A., Sone, T., Harada, T., Curiel, D. T., Kuroki, M., and Nakanishi, Y. (2008) Tumor targeting carboxylesterase fused with anti-CEA scFv improve the anticancer effect with a less toxic dose of irinotecan. *Cancer Gene Ther. 15*, 94–100.

(12) Kortt, A. A., Dolezal, O., Power, B. E., and Hudson, P. J. (2001) Dimeric and trimeric antibodies: high avidity scFvs for cancer targeting. *Biomol. Eng. 18*, 95–108.

(13) Adams, G. P., Tai, M. S., McCartney, J. E., Marks, J. D., Stafford, W. F., 3rd., Houston, L. L., Huston, J. S., and Weiner, L. M. (2006) Avidity-mediated enhancement of in vivo tumor targeting by single-chain Fv dimers. *Clin. Cancer Res. 12*, 1599–605.

(14) Behr, T. M., Gotthardt, M., Becker, W., and Behe, M. (2002) Radioiodination of monoclonal antibodies, proteins and peptides for diagnosis and therapy. A review of standardized, reliable and safe procedures for clinical grade levels kBq to GBq in the Gottingen/Marburg experience. *Nuklearmedizin 41*, 71–9.

(15) Nikula, T. K., Bocchia, M., Curcio, M. J., Sgouros, G., Ma, Y., Finn, R. D., and Scheinberg, D. A. (1995) Impact of the high tyrosine fraction in complementarity determining regions: measured and predicted effects of radioiodination on IgG immunoreactivity. *Mol. Immunol. 32*, 865–72.

(16) McCartney, J. E., Tai, M. S., Hudziak, R. M., Adams, G. P., Weiner, L. M., Jin, D., Stafford, W. F., 3rd., Liu, S., Bookman, M. A., and Laminet, A. A. (1995) Engineering disulfide-linked single-chain Fv dimers [(sFv′)2] with improved solution and targeting properties: anti-digoxin 26−10 (sFv′)2 and anti-c-erbB-2 741F8 (sFv′)2 made by protein folding and bonded through C-terminal cysteinyl peptides. *Protein Eng. 8*, 301–14.

(17) Adams, G. P., McCartney, J. E., Tai, M. S., Oppermann, H., Huston, J. S., Stafford, W. F., 3rd., Bookman, M. A., Fand, I., Houston, L. L., and Weiner, L. M. (1993) Highly specific in vivo tumor targeting by monovalent and divalent forms of 741F8 anti-c-erbB-2 single-chain Fv. *Cancer Res. 53*, 4026–34.

(18) George, A. J., Jamar, F., Tai, M. S., Heelan, B. T., Adams, G. P., McCartney, J. E., Houston, L. L., Weiner, L. M., Oppermann, H., and Peters, A. M. (1995) Radiometal labeling of recombinant proteins by a genetically engineered minimal chelation site: technetium-99m coordination by single-chain Fv antibody fusion proteins through a C-terminal cysteinyl peptide. *Proc. Natl. Acad. Sci. U.S.A. 92*, 8358–62.

(19) Yang, K., Basu, A., Wang, M., Chintala, R., Hsieh, M. C., Liu, S., Hua, J., Zhang, Z., Zhou, J., Li, M., Phyu, H., Petti, G.,

Mendez, M., Janjua, H., Peng, P., Longley, C., Borowski, V., Mehlig, M., and Filpula, D. (2003) Tailoring structure-function and pharmacokinetic properties of single-chain Fv proteins by site-specific PEGylation. *Protein Eng. 16*, 761–70.

(20) Weng, K. C., Noble, C. O., Papahadjopoulos-Sternberg, B., Chen, F. F., Drummond, D. C., Kirpotin, D. B., Wang, D., Hom, Y. K., Hann, B., and Park, J. W. (2008) Targeted tumor cell internalization and imaging of multifunctional quantum dot-conjugated immunoliposomes in vitro and in vivo. *Nano Lett. 8*, 2851–7.

(21) Messerschmidt, S. K., Kolbe, A., Muller, D., Knoll, M., Pleiss, J., and Kontermann, R. E. (2008) Novel single-chain Fv′ formats for the generation of immunoliposomes by site-directed coupling. *Bioconjugate Chem. 19*, 362–9.

(22) Carmichael, J. A., Power, B. E., Garrett, T. P., Yazaki, P. J., Shively, J. E., Raubischek, A. A., Wu, A. M., and Hudson, P. J. (2003) The crystal structure of an anti-CEA scFv diabody assembled from T84.66 scFvs in V(L)-to-V(H) orientation: implications for diabody flexibility. *J. Mol. Biol. 326*, 341–51.

(23) Olafsen, T., Cheung, C. W., Yazaki, P. J., Li, L., Sundaresan, G., Gambhir, S. S., Sherman, M. A., Williams, L. E., Shively, J. E., Raubitschek, A. A., and Wu, A. M. (2004) Covalent disulfide-linked anti-CEA diabody allows site-specific conjugation and radiolabeling for tumor targeting applications. *Protein Eng. Des. Sel. 17*, 21–7.

(24) Bebbington, C., Renner, G., Thomson, S., King, D., Abrams, D., and Yarranton, G. T. (1992) High-level expression of a recombinant antibody from myeloma cells using a glutamine synthetase gene as an amplifiable selection marker. *Biotechnology 10*, 169–175.

(25) Yazaki, P. J., Shively, L., Clark, C., Cheung, C. W., Le, W., Szpikowska, B., Shively, J. E., Raubitschek, A. A., and Wu, A. M. (2001) Mammalian expression and hollow fiber bioreactor production of recombinant anti-CEA diabody and minibody for clinical applications. *J. Immunol. Methods 253*, 195–208.

(26) Golay, J., Cittera, E., Di Gaetano, N., Manganini, M., Mosca, M., Nebuloni, M., van Rooijen, N., Vago, L., and Introna, M. (2006) The role of complement in the therapeutic activity of rituximab in a murine B lymphoma model homing in lymph nodes. *Haematologica 91*, 176–83.

(27) Pietras, R. J., Arboleda, J., Reese, D. M., Wongvipat, N., Pegram, M. D., Ramos, L., Gorman, C. M., Parker, M. G., Sliwkowski, M. X., and Slamon, D. J. (1995) HER-2 tyrosine kinase pathway targets estrogen receptor and promotes hormone-independent growth in human breast cancer cells. *Oncogene 10*, 2435–46.

(28) Carter, P., Presta, L., Gorman, C. M., Ridgway, J. B., Henner, D., Wong, W. L., Rowland, A. M., Kotts, C., Carver, M. E., and Shepard, H. M. (1992) Humanization of an anti-p185HER2 antibody for human cancer therapy. *Proc. Natl. Acad. Sci. U.S.A. 89*, 4285–9.

(29) Barrett, T., Koyama, Y., Hama, Y., Ravizzini, G., Shin, I. S., Jang, B. S., Paik, C. H., Urano, Y., Choyke, P. L., and Kobayashi, H. (2007) In vivo diagnosis of epidermal growth factor receptor expression using molecular imaging with a cocktail of optically labeled monoclonal antibodies. *Clin. Cancer Res. 13*, 6639–48.

(30) Koyama, Y., Hama, Y., Urano, Y., Nguyen, D. M., Choyke, P. L., and Kobayashi, H. (2007) Spectral fluorescence molecular imaging of lung metastases targeting HER2/neu. *Clin. Cancer Res. 13*, 2936–45.

(31) Natarajan, A., Xiong, C. Y., Albrecht, H., DeNardo, G. L., and DeNardo, S. J. (2005) Characterization of site-specific ScFv PEGylation for tumor-targeting pharmaceuticals. *Bioconjugate Chem. 16*, 113–21.

(32) Lee, L. S., Conover, C., Shi, C., Whitlow, M., and Filpula, D. (1999) Prolonged circulating lives of single-chain Fv proteins conjugated with polyethylene glycol: a comparison of conjugation chemistries and compounds. *Bioconjugate Chem. 10*, 973–81.

(33) Venisnik, K. M., Olafsen, T., Loening, A. M., Iyer, M., Gambhir, S. S., and Wu, A. M. (2006) Bifunctional antibody-Renilla luciferase fusion protein for in vivo optical detection of tumors. *Protein Eng. Des. Sel. 19*, 453–60.

(34) Venisnik, K. M., Olafsen, T., Gambhir, S. S., and Wu, A. M. (2007) Fusion of Gaussia luciferase to an engineered anti-carcinoembryonic antigen (CEA) antibody for in vivo optical imaging. *Mol. Imaging Biol. 9*, 267–77.

(35) Michalet, X., Pinaud, F. F., Bentolila, L. A., Tsay, J. M., Doose, S., Li, J. J., Sundaresan, G., Wu, A. M., Gambhir, S. S., and Weiss, S. (2005) Quantum dots for live cells, in vivo imaging, and diagnostics. *Science 307*, 538–44.

(36) Alexis, F., Rhee, J. W., Richie, J. P., Radovic-Moreno, A. F., Langer, R., and Farokhzad, O. C. (2008) New frontiers in nanotechnology for cancer treatment. *Urol. Oncol. 26*, 74–85.

(37) Kam, N. W., O'Connell, M., Wisdom, J. A., and Dai, H. (2005) Carbon nanotubes as multifunctional biological transporters and near-infrared agents for selective cancer cell destruction. *Proc. Natl. Acad. Sci. U.S.A. 102*, 11600–5.

(38) Zheng, G., Patolsky, F., Cui, Y., Wang, W. U., and Lieber, C. M. (2005) Multiplexed electrical detection of cancer markers with nanowire sensor arrays. *Nat. Biotechnol. 23*, 1294–301.

(39) Gruner, G. (2006) Carbon nanotube transistors for biosensing applications. *Anal. Bioanal. Chem. 384*, 322–35.

BC800113V